Materials Research. 2023; 26: e20220433
DOI: https://doi.org/10.1590/1980-5373-MR-2022-0433

Evaluation of Fully Biodegradable PLA/PHB Blend Filled with Microcrystalline Celluloses

***Gisele C. Valle Iulianelli*[a*], *Lucas Viana Costa*[a], *Paulo Sérgio Cruz da Silva*[a],**

***Fernanda Abbate dos Santos*[a]**

[a]*Universidade Federal do Rio de Janeiro, Instituto de Macromoléculas Professora Eloisa Mano, Av. Horácio Macedo 2030, Centro de Tecnologia, Bloco J, Ilha do Fundão, Rio de Janeiro, RJ, Brasil.*

Received: September 26, 2022; Revised: February 16, 2023; Accepted: March 19, 2023

In this work, biodegradable biocomposites were developed using PLA/PHB blend as matrix and two types of microcrystalline cellulose as filler at three different contents. The biocomposites were evaluated regarding their thermal and morphological characteristics and molecular dynamic behavior. It was seen that cellulose addition did not promote significant changes in the *Tm, Tc* and *Tcc* in the matrix. On the other hand, XRD and TGA revealed that the addition of the highest content (7 wt%) of cellulose fillers resulted in a more significant decrease in crystallinity and thermal stability of the PLA/PHB matrix, suggesting a formation of filler aggregates. This indication was confirmed by TD-NMR, whose results pointed to a greater heterogeneity molecular in the samples containing higher cellulose contents. Therefore, this technique proved to be a relevant and complementary tool for the characterization of composites materials, contributing to determinate the most appropriate filler content introduced in a polymer matrix.

Keywords: *PLA/PHB blend, microcrystalline cellulose, biocomposites, TGA, DSC, XRD, TD-NMR.*

1. Introduction

Biodegradable polymers from renewable resources are the most promising alternative to replace conventional petrochemical polymers and minimize the environmental impacts caused by them, such as the accumulation of plastic waste in landfills and their penetration and contamination in the form of microplastics into the whole ecosystem[1]. For this reason, research related to the development of fully biodegradable "green" materials has increased massively in recent years[2].

This class of polymers has many relevant advantages over those conventionally obtained from petroleum, such as biodegradability, biocompatibility, low toxicity, sustainability, among others[3,4]. However, the wide application of these polymers is still a challenge due to inherent limitations on their performance compared to conventional polymers, which in general exhibit superior mechanical properties and thermal stability[5]. These limitations can restrict their use to short-term and single-use applications, such as food packaging.

Among the biodegradable polymers, the aliphatic polyesters are the most attractive due to their good mechanical properties, processability and the ability to undergo both hydrolytic degradation and biodegradation by soil microorganisms in compost[6]. Poly(lactic acid) (PLA) and poly(hydroxyalkanoates) (PHAs) such as Poly(3-hydroxybutyrate) (PHB) are examples of these materials and typify biodegradable polymers derived from renewable resources. Furthermore, both of them are commercialized at large scale, therefore they are suitable candidates for the development of materials that demand high production volume, such as for packing applications.

Polylactic acid or polylactide (PLA) is an aliphatic thermoplastic polyester produced from renewable resources. It is a biodegradable polymer[7-10] that has been employed for various applications, i.e. biomedical, packaging, textile fibers and technical items[7]. PLA is industrially obtained through the polymerization of lactic acid (LA) or by the ring-opening polymerization (ROP) of lactide (the cyclic dimer of lactic acid, as an intermediate)[7,11,12]. Among its attractive properties, it can be pointed to high transparency, high rate of disintegration in compost, ease of processing and ready availability[13]. In addition, PLA exhibits satisfactory mechanical properties (particularly, high tensile strength and Young's modulus and acceptable flexural strength), which are even higher than of many commonly used polymers, such as polystyrene (PS), polypropylene (PP), polyethylene (PE) and others[7,14]. The tensile strength and elastic modulus of PLA are comparable to those of PET, which lead this polymer to a key position in the market of biopolymers, being one of the most promising candidates for further developments in this area. Unfortunately, PLA suffers from some shortcomings, such as being sensitive to moisture, having low-impact strength and being notably brittle, with less than 10% elongation at break and low toughness, which limits its use in applications that demands plastic deformation under high stress[15]. These drawbacks can be surpassed through blending with other polymers and/or through developing bionanocomposites, which can lead to the tuning of their final properties[7].

Several reports in literature have been documenting the blending of PLA with different biodegradable and non-biodegradable polymers, such as poly(ε-caprolactone)[16-18], poly(propylene)[19], poly (ethylene oxide)[20], starch[21], poly

*e-mail: gisele@ima.ufrj.br

(3-hydroxybutyrate)[22], poly(3-hydroxybutyrate-co-3-hydroxyvalerate)[23], polyvinylidene fluoride[24] and poly(butylene adipate-co-terephthalate)[25,26]. When the polymer selected to be blended with PLA is bio-based and/or biodegradable, a new material with low environmental impact is achieved. In this context, PLA/poly-hydroxy butyrate (PHB) blends have attracted great interest, since the combination of these two biopolymers allows the formulation of new biomaterials with enhanced properties as compared to their single components, while maintaining their eco sustainability[27-30].

Poly(3-hydroxybutyrate) (PHB) is an aliphatic polyester with linear polymer chain and it is the predominant polyhydroxyalkanoate (PHA) synthesized by controlled bacterial fermentation[31]. Microbial synthesis of PHB is the preferred method for industrial production because it ensures the proper stereochemistry for biodegradation. Microorganisms synthesize and store PHB when nutrient limited conditions are imposed, while degrading it and metabolizing as the limitation is removed[32,33]. Current production employs *Alcaligenes eutrophus* because it grows efficiently on glucose as a carbon source, accumulates PHB up to 80% of its dry weight, and is able to synthesize polyhydroxybutyrate-co-valerate (PHBV) when propionic acid is added to the feedstock[33].

PHB presents a high degree of crystallinity, which is an important feature to improve PLA's properties, in addition to having superior physical properties over polypropylene for food packaging applications and being completely nontoxic. Furthermore, PHB is optically active, presents a good barrier to permeability of water and gases and exhibits acceptable stability to ultraviolet radiation[34]. On the other hand, it is a brittle polymer, exhibiting inferior low-impact strength, and its poor processability and thermal instability when processed are the foremost drawbacks that limit its industrial usage[30]. The literature proposes the blending, the development of copolymers or the insertion of additives as strategies to improve the mechanical and thermal properties of PHB[34]. Another alternative is the development of PHB nanocomposites due to the potential for improving their properties[35].

Several studies describe PLA/PHB blend as a valuable approach to produce "green" materials, since its properties can be easily modulated through changes in composition. However, some properties still need to be improved to broaden the range of applications. In this context, incorporation of reinforcement materials can promote improvements in this blend properties. Thus, the development of bio-based materials with natural reinforcement fillers, such as cellulose, starch, and chitin, appeals as a promising strategy to provide the enhancement of their properties[36], without interfering with the total biodegradability of the produced material.

Among these fillers, cellulose particularly has been largely employed to produce biocomposites, considering it is the most abundant biopolymer in nature and is available in a wide variety of resources, such as plants and microorganisms. The isolated cellulose should be submitted to a partial acid hydrolysis process to produce microcrystalline cellulose. During the process of acid hydrolysis, the non-crystalline region is preferentially hydrolyzed to produce a cellulosic material with high crystallinity[37] and better mechanical properties.

The purpose of this study was to develop fully biodegradable biocomposites based on the blend of poly(lactic acid) (PLA) and poly(3-hydroxybutyrate) (PHB) filled with microcrystalline cellulose untreated and treated by sonication at 3, 5 and 7 wt% and to characterize the obtained materials by conventional techniques, such as thermogravimetric analysis (TGA), differential scanning calorimetry (DSC) and X-ray diffraction (XRD) and also by a more recent and unconventional technique named time domain-nuclear magnetic resonance (TD-NMR). This characterization provides relevant and complementary information about the molecular dynamic behavior of the materials through the nuclear relaxation measurements such as by spin-lattice relaxation time (T_1H) determination and regarding the homogeneity at molecular level by means of domain distribution curve profile, allowing a more detailed evaluation of the composites systems[38]. Furthermore TD-NMR allows to conduct measurements fast and without any special sample preparation.

2. Materials and Methods

2.1. Materials

The materials used in this study were supplied as follows: NatureWorks™ 2002D PLA in pellet from Nature Works; Biocycle®, PHB in powder form from PHB Industrial S.A., Chloroform ($CHCl_3$) from Merck Chemical Company, Microcrystalline cellulose (MCC) ph102 in powder form from Viafarma; and sMCC obtained from MCC by sonication treatment.

2.2. Preparation of the microcrystalline cellulose

The sMCC (sonicated MCC) was produced from MCC aqueous suspensions at a concentration of 1 wt% by subjecting them to high intensity ultrasonication treatment. The suspensions were exposed to ultrasonication for 60 min at 25 ºC in order to modify the cellulosic material's crystalline structure by size reduction and shape modification of its crystallites. Afterwards, the ultrasound irradiated suspensions were freeze-dried for 48 h to obtain powdered sMCC. The procedure was carried out in Eco-sonics equipment from Ultronique Company, Disruptor model, at a frequency of 20 kHz and potency of 500 W.

2.3. Preparation of the blended biocomposites systems

The blended polymeric films were prepared by the solution casting method using $CHCl_3$ as solvent. Two different series of materials were obtained by this method, both based on a blended polymeric matrix made of PLA and PHB. These series differ in the reinforcement filler type added to them. The first series was reinforced with MCC, used as received, and the second one with sMCC (sonicated MCC).

For the formulation of each film, PLA and PHB at a ratio of 3:1 (wt%) were solubilized simultaneously in chloroform ($CHCl_3$) under vigorous magnetic stirring for 24 hours at room temperature, resulting in a 10% w/v solution. Formulations for

neat PLA and PHB were also prepared by the same method for the production of individual films of each polymer.

Afterwards, MCC or sMCC were systematically added to chloroform in three different proportions, resulting in three dispersions of each cellulosic filler, appropriate to produce films with 3, 5, and 7 wt% (filler/polymers blend). In this procedure, the cellulosic fillers were dispersed in chloroform by magnetic stirring at room temperature for 30 min, followed by a sonication bath for another 30 min. Subsequently, each polymer blend solution was added to each cellulosic filler suspension and kept under constant magnetic stirring for an additional hour. The resulting mixtures were cast into glass Petri dishes and placed in the fume hood for at least three days to evaporate all residual solvent. A polymer blend film without cellulose fillers was also prepared by this method. The produced films were coded as described in Table 1.

2.4. Characterization of the microcrystalline cellulose fillers

The morphology of MCC and sMCC samples was investigated by Scanning Electron Microscopy (SEM). For the sample preparation, each cellulosic material in powder form was individually placed on a double-sided carbon tape and gold coated for 4 min in sputtering. The equipment used for this analysis was a Hitachi TM3030 Plus Scanning Electron Microscope at an accelerating voltage of 1-15 kV.

2.5. Characterization of the blended biocomposites systems

The characteristics and properties of the blended biocomposites systems were evaluated by X-ray Diffraction (XRD), Thermogravimetric Analysis (TGA), Differential Scanning Calorimetry (DSC), and Time Domain-Nuclear Magnetic Resonance (TD-NMR). The analyses were performed as described below.

XRD was performed using Rigaku Ultima IV diffractometer with CuKα radiation generator (λ=0.154 nm, 40Kv, 120 mA) at room temperature, in the range of 2θ from 2° to 40° at a rate of 1°/min, and step of 0.05°. This technique was used to evaluate the crystalline profile of the materials. Their crystallinity degrees were determined using Origin® software, according to the equation X_C (%) = I_C / (I_C + I_A) x 100, where Xc is the crystallinity degree; Ic is the sum of the areas under the crystalline peaks and I_A is the area of the amorphous halo. The peaks were deconvoluted using Gaussian peak function.

DSC analyses were carried out using a TA Instruments Q1000 calorimeter (with a temperature accuracy of ±2 ºC) under a nitrogen flow rate of 50 mL/min. The samples were subjected to a first heating ramp from –30 to 200 ºC, followed by a cooling ramp from 200 to –30 ºC. After this heating/cooling cycle, the samples were subjected to a second heating ramp from –30 to 200 ºC. The heating and cooling ramps were all performed at a scanning rate of 10 ºC/min. The crystallization temperature (*T*c), cold crystallization temperature (*T*cc) and melting temperature (*T*m) were determined from second cooling and second heating scans. The first heating ramp was used only to erase the polymer thermal history.

TGA measurements were performed using a TA Instruments Q500 calorimeter (with a temperature accuracy of ±2 ºC). The samples were placed in a platinum holder under continuous nitrogen flow and heated at the rate of 10 ºC/min from 20 to 700 ºC. This analytical technique was used to investigate the thermal stability of the produced materials. From TGA two parameters were measured to study the thermal stability of the prepared materials: the initial degradation temperature (Tonset) and temperature of maximum degradation rate (Tmax). The Tonset values were obtained from TG curves and denote the lowest temperature at which mass variation of the material occurs. In turn, the Tmax values were obtained from the peak of each DTG curve, which refers to the temperature where the degradation speed occurs more sharply.

TD-NMR analyses were performed using a low-field NMR spectrometer Maran Ultra operating at 23 MHz, employing an inversion-recovery pulse sequence (recycle delay - 180º- τ - 90º - acquisition time). The analysis was carried out at 27 °C; with τ values varying from 0.01 to 10,000 ms and recycle interval of 3 s, utilizing 40 points with 4 accumulations. The equipment was operated to determine the spin-lattice relaxation times of the hydrogen nucleus (T_1H) and the distribution domain curves. The spin-lattice relaxation times were obtained with the aid of the WinFit program and the distribution domain curves were fitted with the WinDXP software.

3. Results and Discussion

3.1. Characterization of the microcrystalline cellulose fillers

SEM analyses were performed to investigate MCC morphology and describe possible changes after the

Table 1. Description and codes of the materials.

Materials' codes	Materials' descriptions
PLA	Unfilled PLA
PHB	Unfilled PHB
PLA/PHB	Unfilled PLA/PHB blend
PLA/PHB MCC3	PLA/PHB blend filled with 3wt% of MCC
PLA/PHB MCC5	PLA/PHB blend filled with 5wt% of MCC
PLA/PHB MCC7	PLA/PHB blend filled with 7wt% of MCC
PLA/PHB sMCC3	PLA/PHB blend filled with 3wt% of sonicated MCC
PLA/PHB sMCC5	PLA/PHB blend filled with 5wt% of sonicated MCC
PLA/PHB sMCC7	PLA/PHB blend filled with 7wt% of sonicated MCC

ultrasonication treatment. Images obtained by SEM for the cellulosic fillers (Figure 1) revealed that the ultrasonication treatment of MCC promoted modifications in the size and shape of the particles. As observed in the SEM images, the MCC particles predominantly presented a more regular morphology with long or rounded structures, having an average particle size around 100 µm (Figures 1A and 1B). On the other hand, sMCC presented reduced size particles, around 25 µm, with shorter structure and irregular morphology compared to the MCC particles (Figures 1C and 1D). Furthermore, the SEM images for sMCC sample exhibited aggregates formed by its thinner particles, as highlighted in Figures 1C and 1D.

3.2. Characterization of the PLA/PHB biocomposites

3.2.1. X-ray diffraction (XRD)

Figure 2 depicts the X-ray diffraction patterns obtained for MCC, sMCC, neat PLA, neat PHB and PLA/PHB blend. The X-ray diffraction patterns of MCC and sMCC showed characteristic peaks related to cellulose at $2\theta = 14.5°$, 16.5°, 22.5° and 35° attributed to the (110), (1-10), (200) and (004) planes, respectively[39]. These peaks are characteristic of cellulose I, which agrees with the work developed by Rong et al.[40].

For the neat PLA film, it was observed an amorphous halo (Figure 2), indicating low degree of crystallinity of this film. This result is expected for PLA films obtained by solution casting method and it is consistent to other reported in the literature[41,42].

The result obtained from XRD analysis for the neat PHB film revealed a crystalline profile corresponding to orthorhombic crystal planes. For this film, two strong scattering intensity peaks were detected at around $2\theta = 13°$ and 17°, which are assigned to the (020) and (110) planes of the orthorhombic unit cell, respectively. Both correspond to the characteristic peaks of PHB crystallinity. Other weaker reflections located at around 22.5°, 26°, 27° and 31° correspond to (111), (121), (040) and (002) planes, respectively. Furthermore, the result of this analysis also showed that the neat PHB film presented a small amount of orthorhombic β-form crystal with zig-zag conformation, as revealed by the reflection of the (021) plane located at $2\theta = 20°$[43]. This result showed that unlike PLA, the solution casting method did not prevent the development of crystallinity in the PHB film.

The XRD pattern of PLA/PHB blend (Figure 2) showed peaks at around 13º, 22.5º, 26º and 27º characteristic to the PHB, but weaker than that found for neat PHB film. Presumably, this decrease in the intensity of the peaks is due to the minor quantity of PHB (25 wt.%) in this blend formulation. For the same reason, it was not possible to identify the peak found in the pattern of the neat PHB film at around 31°. Furthermore, the XRD pattern of the unfilled PLA/PHB showed peaks at 16.9° and 19.3º, both attributed to the PLA phase[44,45]. The very strong reflection at

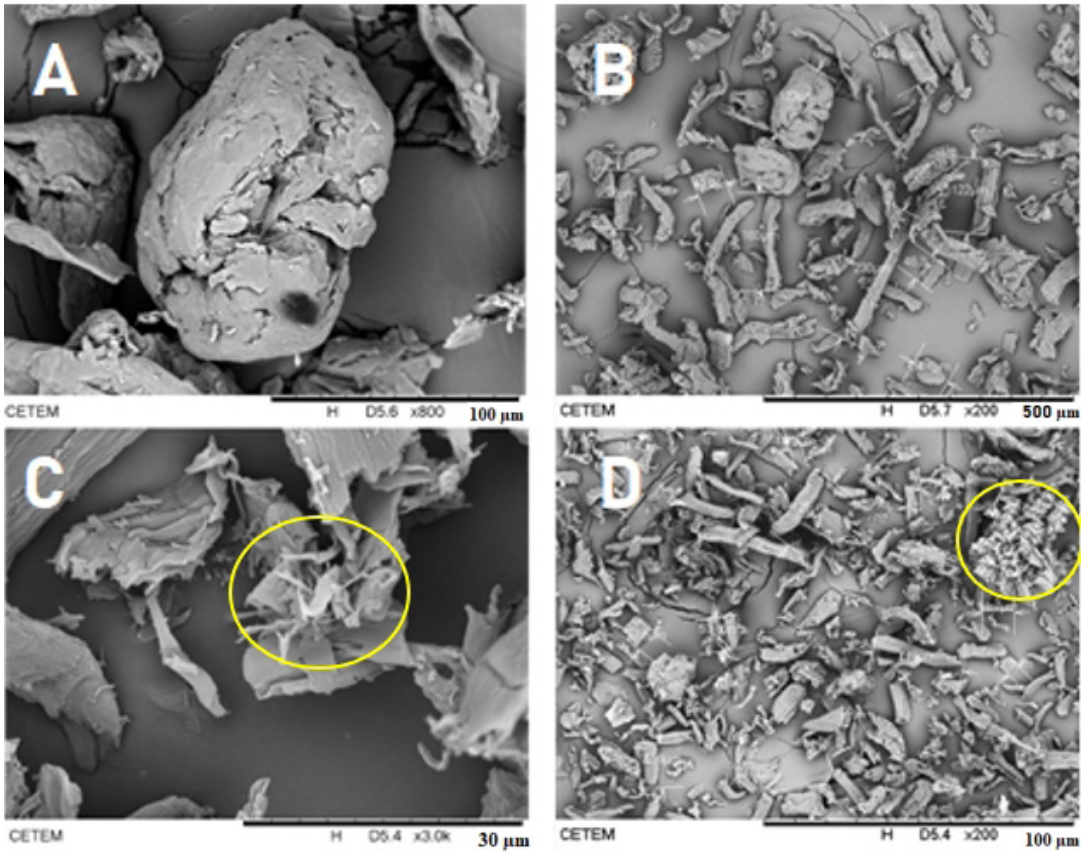

Figure 1. SEM images obtained for MCC (micrographs A and B) and sMCC (micrographs C and D).

2θ = 16.9° corresponds to (110) and/or (200) planes, while the less intense peak at 19.3° is assigned to the reflection of the (203) plane[46,47]. These diffraction peaks indicated that the addition of semi-crystalline PHB induces the PLA's crystallinity, suggesting that PHB acts as a nucleating agent in PLA, which is in accordance with other reports[48-50]. The nucleating effect observed can be attributed to the highly ordered stereochemical structure of PHB crystallizes as small spherulites that are well dispersed in the amorphous PLA matrix and act as nucleating agents for this polymer[50], increasing its crystallinity[51,52].

Regarding to the PLA/PHB biocomposites it was found a similar diffractogram profile compared to PLA/PHB blend unfilled (Fig. 3), but it was also possible to identify a more prominent peak at 2θ = 22,5º, suggesting the contribution of the (200) plane of cellulose fillers. Similarly to the observed in the XRD pattern of PHB film, all the PLA/PHB biocomposites samples presented a small amount of orthorhombic β-form crystal with zig-zag conformation, as revealed by reflection at 2θ = 20º. Compared to the PLA/PHB unfilled film, PLA/PHB/MMC and PLA/PHB/sMCC systems containing 7 wt.% of cellulose filler presented a slight reduction in the peak intensity at 16.9º, suggesting changes in the crystalline profile of the matrix (Figure 3A and Figure 3B).

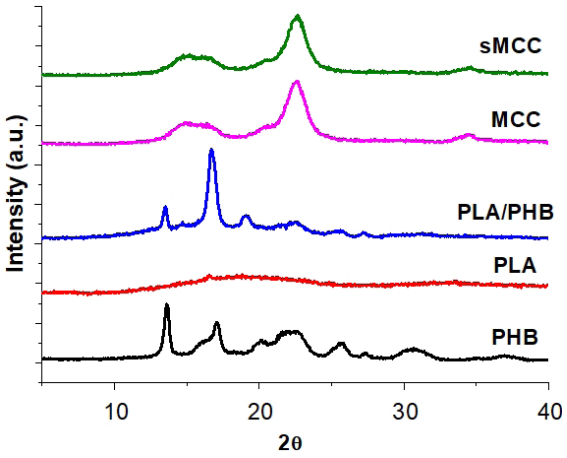

Figure 2. XRD diffractograms obtained for neat PHB, neat PLA, PLA/PHB blend, MCC and sMCC.

Regarding degree of crystallinity, it was found values of 49% for PLA/PHB unfilled, while PLA/PHB biocomposites containing 3%, 5% and 7% of MCC filler presented values of 43%, 42% and 38%, respectively and PLA/PHB biocomposites containing 3%, 5% and 7% of sMCC exhibited values of 46%, 45%, and 41%, respectively. This result showed that the progressive addition of both MCC and sMMC fillers promoted a gradual decrease in the crystallinity of the matrix. However, comparing the materials with the same cellulosic filler content, the crystallinity values of the films containing sMCC were higher than those found for the films with MCC. This result suggests that MCC and sMCC have a slightly different influence on the crystalline profile of the PLA/PHB matrix. This effect can be related to the different morphologies of these cellulosic fillers. The sMCC particles presented shorter structures than the MCC ones, which indicates that sMCC has a higher specific surface area. This characteristic of sMCC probably contributes to increasing the contact area between the surface of sMCC particles and the polymers. Thus, the most pronounced effect on the crystalline profile of PLA/PHB matrix was promoted by sMCC incorporation, which is possibly related to the more effective interaction between both phases in the biocomposites.

3.2.2. Differential scanning calorimetry (DSC)

The data obtained by DSC for neat PLA, neat PHB, PLA/PHB blend; PLA/PHB/MCC biocomposites and PLA/PHB/sMCC biocomposites are denoted in Table 2. The parameters include: melting temperature (*Tm*); melting enthalpy (ΔHm), crystallization temperature (*Tc*) and cold crystallization temperature (*Tcc*). For this discussion, *Tm1* refers to the main melting temperature peak found for both PLA and PHB and the melting enthalpy (ΔHm1) corresponds to the *Tm1*. In addition, *Tm2* and *Tcc1*were exclusively related to the PLA phase, while *Tcc2* was related to the PHB phase.

Regarding unfilled polymer materials, the results showed that neat PLA did not crystallize during cooling, thus it did

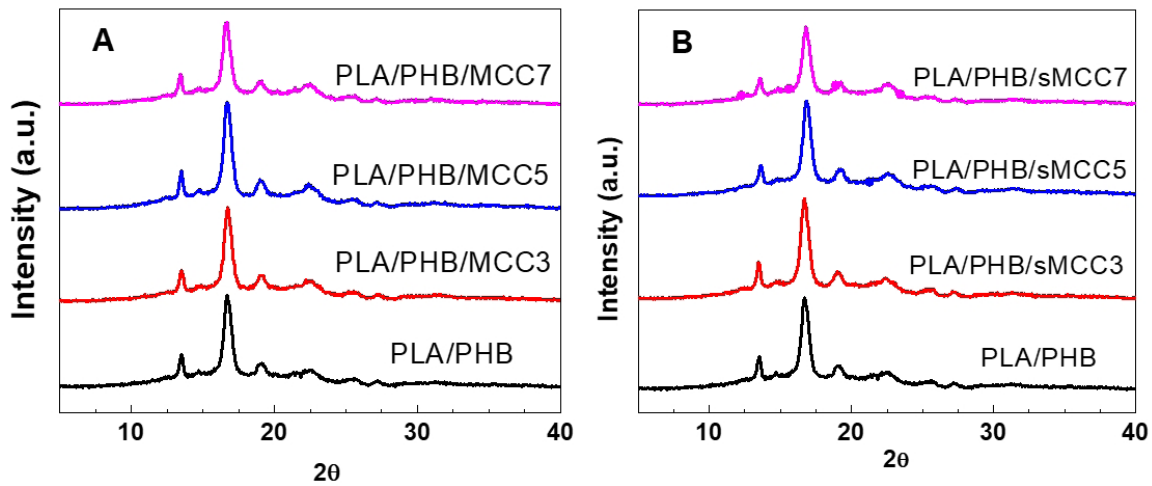

Figure 3. XRD diffractograms obtained for biocomposites systems containing MCC (A) and sMCC (B).

not present crystallization temperature (*Tc*) as was also observed in other studies[53,54]. On the other hand, it was possible to identify a crystallization event on heating (cold crystallization, *Tcc1*) at 99 ºC (Table 2). Furthermore, PLA presented two melting temperatures: *Tm1* with an intense endothermic peak at 174 ºC related to α crystal form and *Tm2* with an almost inconspicuous peak at 160 ºC referred to β crystal form. The melting temperature of the α-form is higher because of the better quality and higher size of its crystals[54].

Concerning the PHB it was found a notable exothermic peak during cooling at 65 ºC related to crystallization temperature (*Tc*), while *Tm* was detected at 174 ºC. Moreover, it was identified an exothermic peak during the second heating due to the cold crystallization temperature at 48 ºC (*Tcc2*). This parameter was also reported elsewhere[55].

PLA/PHB blend, as well PLA, did not present *Tc*, showing that PHB addition did not favor the crystallization on cooling. This sample presented only cold crystallization temperatures: *Tcc2* at 46 ºC related to the PHB phase; and *Tcc1* at 95 ºC related to the PLA phase. Ultimately, the *Tm1* was found at 174 ºC (Table 2).

For the developed biocomposites, except for PLA/PHB/MCC5 and PLA/PHB/sMCC3, it was observed that both MCC and sMCC induced crystallization on cooling (*Tc*). This result indicates that the microcrystalline cellulose fillers used in this study can act as nucleating agent for this crystallization mode. The addition of fillers promoting a nucleating effect for PLA has been reported in other studies[53,56]. Regarding melting temperature (*Tm*), the addition of MCC and sMCC at any of three proportion maintained the values found for PLA/PHB blend (Table 2).

3.2.3. Thermogravimetric analysis (TGA)

TGA analysis is a very useful tool to investigate the thermal stability of materials. In this study, two parameters were measured to evaluate the thermal behavior of the prepared biocomposite systems and then compare them to the PLA/PHB unfilled matrix. The first parameter obtained from TG curves was the Tonset value, which represents the lowest temperature at which mass variation of the material occurs. The second parameter was the Tmax value obtained from the DTG peak, related to the temperature of maximum degradation rate.

Comparing the thermal stability profile of neat PLA and neat PHB, it was observed that both materials presented a single-step thermal degradation (Figure 4). However, PLA had a higher thermal stability than PHB with Tonset at 314 ºC and Tmax at 345 ºC, while PHB showed Tonset at 256 ºC and Tmax at 270 ºC (Table 3). Regarding the PLA/PHB blend, it was observed that the addition of PHB caused changes on the thermal degradation profile. The TGA curves of the PLA/PHB blend revealed a two-stage degradation. The first step of mass loss was attributed to the degradation of PHB and the second stage was related to PLA, as also described elsewhere[57]. For this reason, it was named Tonset 1 and

Table 2. Thermal data obtained by DSC for PLA, PHB. PLA/PHB blend and their biocomposites systems.

Materials	*Tm1* (˚C)	*Tm2* (ºC)	ΔHm1 (J/g)	*Tc* (˚C)	*Tcc1* (˚C)	*Tcc2* (˚C)
PLA	174	160	48	ND	99	-----
PHB	174	------	97	65	-----	48
PLA/PHB	174	159	42	ND	95	46
PLA/PHB/MCC3	174	159	39	70	96	46
PLA/PHB/ MCC5	174	159	43	ND	96	46
PLA/PHB/ MCC7	174	159	43	68	96	46
PLA/PHB/ sMCC3	174	160	36	ND	96	45
PLA/PHB/sMCC5	174	159	40	68	96	45
PLA/PHB/ sMCC7	174	159	39	65	96	45

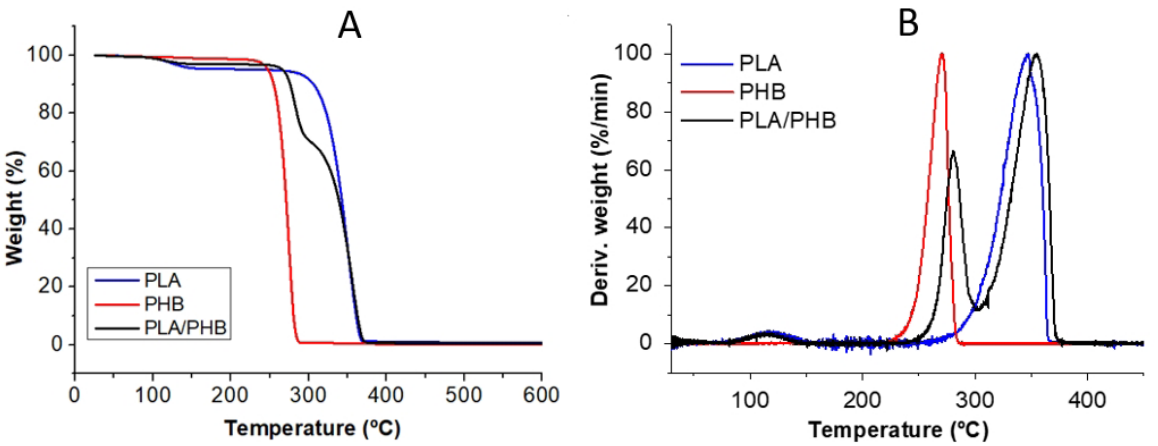

Figure 4. TG curves (A) and DTG curves (b) obtained for neat PLA, neat PHB and PLA/PHB blend.

Tmax 1 for temperatures related to PHB phase and Tonset 2 and Tmax 2 for those concerning to PLA phase. PLA/PHB blend presented Tonset 1 and Tmax 1 at 270 ºC and 280 ºC, respectively and Tonset 2 and Tmax 2 at 320 ºC at 354 ºC, respectively (Figures 4A and 4B). Considering the thermal decomposition of the PLA and PHB phases separately, it was possible to observe a slight increase in the thermal stability of both phases in the blend, so that Tonset 1 and Tonset 2, as well as Tmax 1 and Tmax 2 presented higher values in the PLA/PHB blend compared to the values found for neat PLA and PHB (Table 3 and Figure 4B).

For the biocomposites, MCC addition at 3 and 5 wt% did not cause a significant change in the thermal stability of the PLA/PHB matrix, maintaining Tonset 1, Tonset 2, Tmax 1 and Tmax 2 practically unchanged. On the other hand, the addition of 7 wt% of MCC promoted a significant decrease on the thermal performance of the PLA/PHB matrix, with a decrease of 35 °C and 27 ºC in the Tonset 1 and Tmax 1, respectively and of 19 ºC and 36 ºC on the Tonset 2 and Tmax 2, respectively (Table 3, Figure 5A and Figure 5B).

For biocomposites prepared with sMCC, the effect of filler addition was slightly different. For these systems, it was observed a decrease in the thermal stability for all formulations, but in the same way as was seen for the formulations containing MCC, for PLA/PHB/sMCC formulation containing 7 wt% of filler was observed a more significant decrease on the thermal stability. For this formulation, there was a decrease of 23 ºC and 18 ºC related to Tonset 1 and Tmax 1, respectively and of 15 ºC and 32 ºC on the Tonset 2 and Tmax 2, respectively (Table 3, Figure 6A and Figure 6B). The results obtained by TGA suggest that the addition of 7 wt% of microcrystalline celluloses, regardless of the type, resulted in a more heterogeneous systems with weaker interactions between the polymer and filler phases.

3.2.4. Time Domain-Nuclear Magnetic Resonance (TD-NMR)

The proton spin-lattice relaxation time (T_1H) and the domain curves of the samples were obtained by an unconventional TD-NMR technique, using a low-field NMR equipment. The obtained parameters by TD-NMR provide important information about dynamic molecular behavior of materials such as polymers and their composites and nanocomposites[58]. The determination of the nuclear relaxation parameters can be exploited to discriminate different dynamical regimes inside the material, depending on its structure and morphology. Motional correlation times affect, in turn, macroscopic dynamical behavior, related to viscoelasticity, mechanical response, and processing characteristics[59]. T_1H measurements inform about the mobility of the sample at the molecular level, so that higher T_1H values mean lower molecular mobility. Domain curves provide information about the homogeneity of materials at the molecular level, according to the number of curves present in the plot and these curves' base width.

Table 3. TGA data obtained for PHB, PLA, PLA/PHB blend and their biocomposites systems.

Materials	Tonset 1 (˚C)	Tonset 2 (˚C)	Tmax 1 (˚C)	Tmax 2 (˚C)
PLA	------	314	------	345
PHB	256	------	270	------
PLA/PHB	270	320	280	354
PLA/PHB MCC3	269	317	282	346
PLA/PHB MCC5	272	322	285	349
PLA/PHB MCC7	235	301	253	318
PLA/PHB sMCC3	261	316	277	334
PLA/PHB sMCC5	259	319	274	335
PLA/PHB sMCC7	247	305	262	322

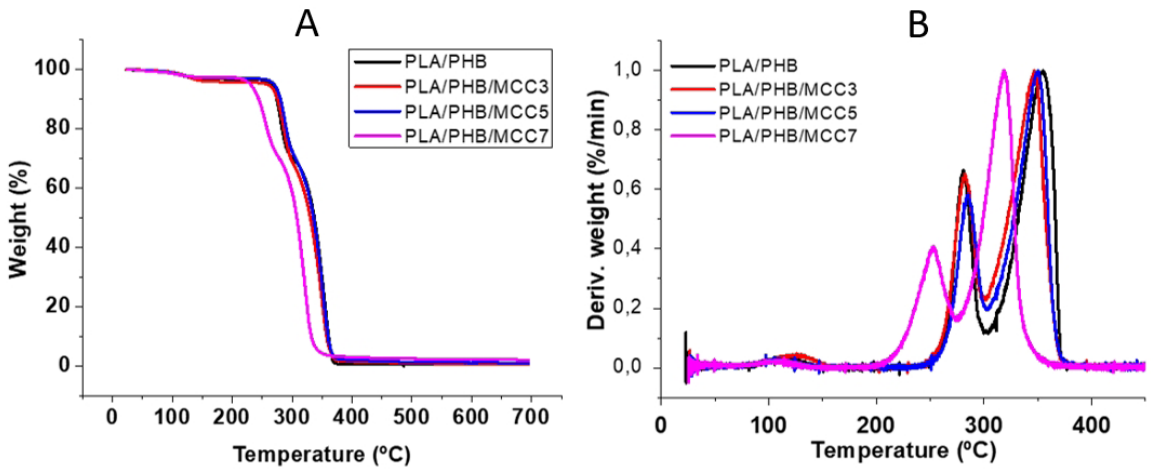

Figure 5. TG curves (A) and DTG curves (b) obtained for PLA/PHB/MCC biocomposite systems.

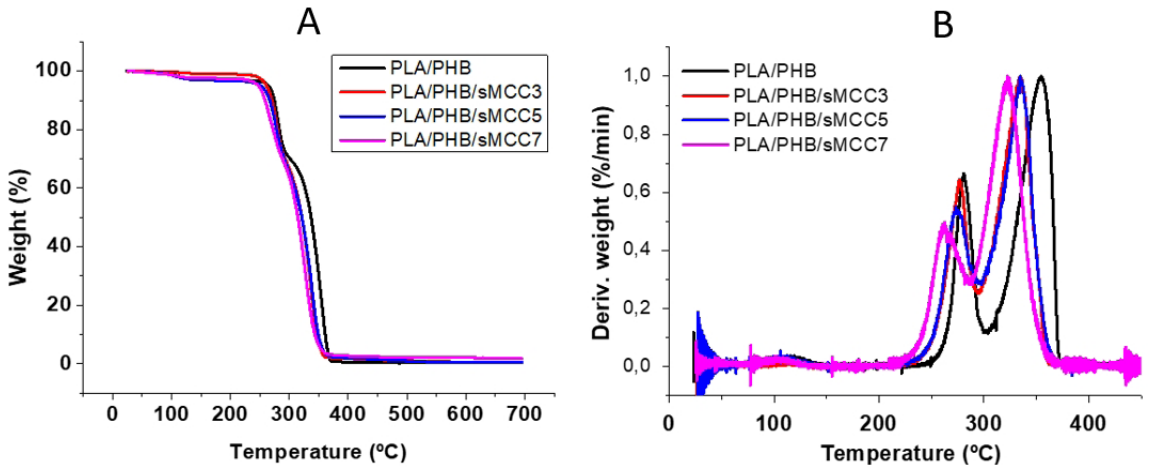

Figure 6. TG curves (A) and DTG curves (b) obtained for PLA/PHB/sMCC biocomposite systems.

For this parameter, fewer domain curves and narrower baseline of curves mean a more homogeneous material[60].

Figure 7 shows the results obtained from TD-NMR analysis for neat PLA, neat PHB and PLA/PHB blend. Regarding T_1H values, it was found that PLA presented a spin-lattice relaxation time at 724 ms, PHB at 643 ms and PLA/PHB blend at 693 ms. The highest T_1H relaxation time found for PLA indicates that this sample has lower molecular mobility. Furthermore, it was seen that PHB incorporation into PLA to develop the blend increased the molecular mobility of this system, so a less brittle material is expected. In relation to the domain curve plot, it was noted that the PLA/PHB blend presented a wider base of the domain curve, indicating a greater molecular heterogeneity of this sample compared to isolated PLA and PHB, as expected, since it is an immiscible polymer blend.

For all PLA/PHB systems containing MCC or sMCC, regardless of filler ratio, it was observed a decrease in the T_1H values compared to the unfilled PLA/PHB matrix (Figures 8A and 8B), which indicates a reduction of the inter- and intramolecular interaction within the polymer chains promoted by filler distribution in the matrix.

Analyzing the systems separately, for PLA/PHB/MCC systems it was found T_1H values at 663 ms, 664 ms and 613 ms for systems containing 3, 5 and 7 wt% of MCC, respectively. Compared to the T_1H value of the unfilled PLA/PHB (693 ms), it was inferred that the addition of MCC similarly increased the molecular mobility of the systems containing 3 and 5 wt.% of filler. For the system containing the highest MCC proportion (PLA/PHB/MCC7), the change was more significant, indicating the greater molecular mobility found among PLA/PHB/MCC systems. From domain curves, it was possible to observe that the addition of MCC at 3 wt% in the PLA/PHB matrix promoted a higher homogeneity at molecular level, as can be seen by a narrowest domain baseline found for PLA/PHB/MCC3 system, compared to other samples, including the unfilled PLA/PHB.

For the PLA/PHB/sMCC systems, were found T_1H values at 653 ms, 635 ms and 611 ms for systems containing 3, 5 and 7 wt% of sonicated microcrystalline cellulose (sMCC),

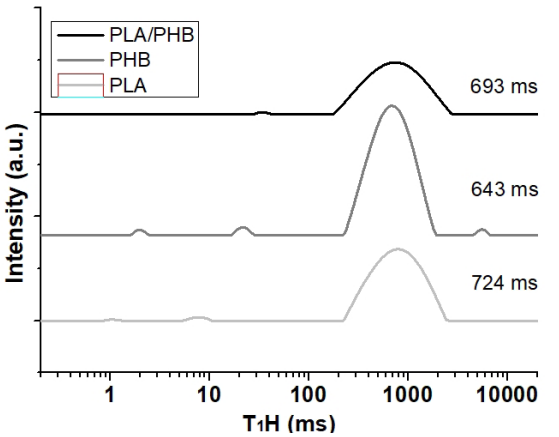

Figure 7. Distribution domain curves for the PLA, PHB and PLA/PHB blend.

respectively. This result showed a slightly different behavior compared to those observed for the systems prepared with MCC. For the PLA/PHB/sMCC systems, it was seen a progressive decrease in the T_1H values with increase of sMCC. This behavior indicates that the increasing addition of sMCC reduces progressively the molecular rigidity of the PLA/PHB matrix. In relation to the data obtained from the domain curves, it was seen that the increasing addition of sMCC disfavors the homogeneity of the system, as the domain curves become progressively wider or new domains appear. Similarly, to that observed for PLA/PHB/MCC systems, the sample that showed the greatest molecular homogeneity was the one containing 3wt.% of sMCC and the most heterogeneous system was the one containing 7 wt% of filler.

Comparing the systems prepared with MCC and sMCC at the same filler proportions, it was observed that the systems containing sMCC presented a more significant change, since the T_1H values were lower and the domain distribution curves displayed a wider base curve and/or new minor domains were created, indicating greater heterogeneity.

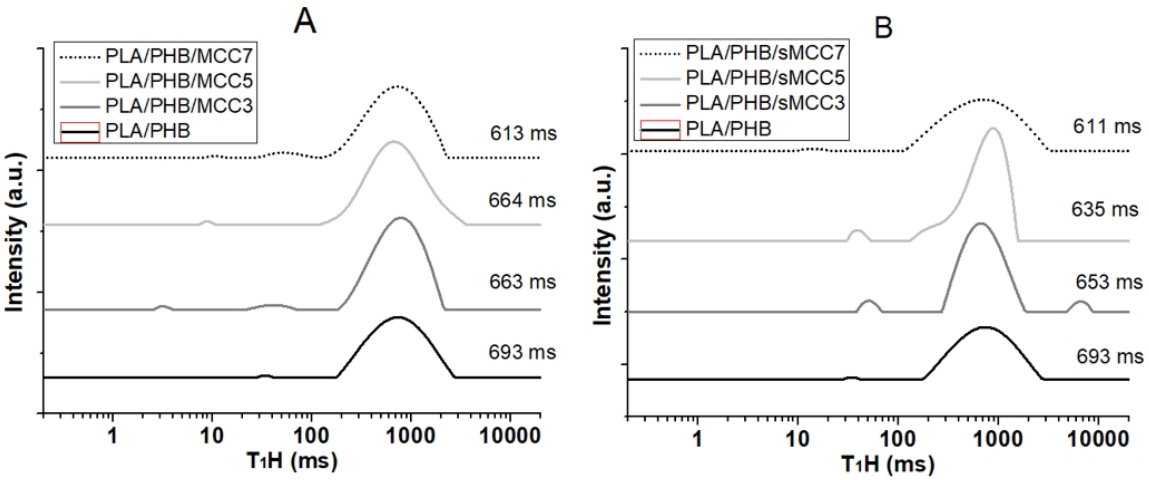

Figure 8. Distribution domain curves for the PLA/PHB biocomposite systems with (A) MCC and (B) sMCC.

The results obtained by TD-NMR corroborated with those found by TGA and by XRD, indicating that the heterogeneity molecular of composites systems can induce a decrease of some properties such as thermal stability and degree of crystallinity of the materials.

4. Conclusions

Biodegradable biocomposites were developed using PLA/PHB blend as matrix and two types of microcrystalline cellulose at 3, 5 and 7 wt% as filler. The influence of the type and content of cellulose filler on the thermal properties and crystallinity parameters of the obtained samples were investigated. In addition, TD-NMR technique was carried out to examine the molecular dynamic behavior and homogeneity at molecular level of the developed materials and investigate a possible correlation of these parameters with the thermal and morphological properties evaluated in this study. Generally, it was found by XRD and TGA that the highest content (7 wt%) of both cellulose fillers caused decrease in the crystallinity degree and in the thermal stability of the PLA/PHB matrix, respectively. TD-NMR analysis provided a more detailed investigation, showing that the PLA/PHB systems containing 7 wt% of MCC or sMCC exhibited greater heterogeneity at molecular level. From this result it was concluded that, despite not interfering in the thermal transition temperatures investigated by DSC, the molecular heterogeneity parameter was related to the decrease in thermal stability and degree of crystallinity of the samples. Thus TD-NMR, which is considered as a fast and non-destructive technique, can be used as an important tool in the characterization of composite materials, assisting in the determination of the best filler content in these materials, based on the evaluation of molecular homogeneity, thus allowing to optimize the final properties of the developed materials.

5. Acknowledgments

The authors gratefully acknowledge the financial support provided by FAPERJ.

6. References

1. Mosnáčková K, Šišková AO, Kleinová A, Danko M, Mosnáček J. Properties and degradation of novel fully biodegradable PLA/PHB blends filled with keratin. Int J Mol Sci. 2020;21(24):1-15.
2. Moshood TD, Nawanir G, Mahmud F, Mohamad F, Ahmad MH, AbdulGhani A. Sustainability of biodegradable plastics: new problem or solution to solve the global plastic pollution? Curr Res Green and Sustain Chem. 2022;5:100273.
3. Mohanty AK, Misra M, Hinrichsen G. Biofibres, biodegradable polymers and biocomposites: an overview. Macromol Mater Eng. 2000;276:1-24.
4. Costa LV, Iulianelli GCV, da Silva PSRC, dos Santos FA. Obtaining and characterization of biodegradable composites reinforced with microcrystalline cellulose fillers. Mater Sci Appl. 2021;12(12):561-77.
5. Harada J, Amorim CA, Braga PL, Machado LDB, Oliveira RR, Cabral L, et al. Characterization of biodegradable mulch black films incorporated with organics fertilizers and rice husk ash. In: Proceedings of the 146th TMS Annual Meeting and Exhibition; 2017; San Diego. USA: TSM.
6. Mosnáčková K, Šlosár M, Kollár J, Janigová I, Šišková A, Chmela Š, et al. Ageing of plasticized poly(lactic acid)/poly(3-hydroxybutyrate)/carbon black mulching films during one season of sweet pepper production. Eur Polym J. 2019;114:81-9.
7. Murariu M, Dubois P. PLA composites: from production to properties. Adv Drug Deliv Rev. 2016;107:17-46.
8. Taib NAAB, Rahman MR, Huda D, Kuok KK, Hamdan S, Bakri MKB et al. A review on poly lactic acid (PLA) as a biodegradable. Polym Bull. 2023;80:1179-213.
9. Chen Y, Lu T, Li L, Zhang H, Wang H, Ke F. Fully biodegradable PLA composite with improved mechanical properties via 3D printing. Mater Lett. 2023;331:133543.
10. Gois GS, Andrade MF, Garcia SMS, Vinhas GM, Santos ASF, Medeiros ES, et al. Soil biodegradation of PLA/CNW nanocomposites modified with ethylene oxide derivatives. Mater Res. 2017;20(Suppl. 2):899-904.
11. Madhavan Nampoothiri K, Nair NR, John RP. An overview of the recent developments in polylactide (PLA) research. Bioresour Technol. 2010;101:8493-501.
12. Vink ETH, Davies S. Life cycle inventory and impact assessment data for 2014 Ingeo® polylactide production. Ind Biotechnol (New Rochelle NY). 2015;11(3):167-80.
13. Arrieta MP, Fortunati E, Dominici F, Rayón E, López J, Kenny JM. Multifunctional PLA-PHB/cellulose nanocrystal films:

processing, structural and thermal properties. Carbohydr Polym. 2014;107(1):16-24.
14. Hamad K, Kaseem M, Yang HW, Deri F, Ko YG. Properties and medical applications of polylactic acid: a review. Express Polym Lett. 2015;9(5):435-55.
15. Rasal RM, Janorkar AV, Hirt DE. Poly(lactic acid) modifications. Prog Polym Sci. 2010;35:338-56.
16. Huang Y, Brünig H, Boldt R, Müller MT, Wießner S. Fabrication of melt-spun fibers from irradiation modified biocompatible PLA/PCL blends. Eur Polym J. 2022;162(5):110895.
17. Herrero-Herrero M, Alberdi-Torres S, González-Fernández ML, Vilariño-Feltrer G, Rodríguez-Hernández JC, Vallés-Lluch A, et al. Influence of chemistry and fiber diameter of electrospun PLA, PCL and their blend membranes, intended as cell supports, on their biological behavior. Polym Test. 2021;103:107364.
18. Lu H, Kazarian SG. How does high-pressure CO2 affect the morphology of PCL/PLA blends? Visualization of phase separation using in situ ATR-FTIR spectroscopic imaging. Spectrochim Acta A Mol Biomol Spectrosc. 2020;243:118760.
19. Hayoune F, Chelouche S, Trache D, Zitouni S, Grohens Y. Thermal decomposition kinetics and lifetime prediction of a PP/PLA blend supplemented with iron stearate during artificial aging. Thermochim Acta. 2020;690:178700.
20. Chaiya N, Daranarong D, Worajittiphon P, Somsunan R, Meepowpan P, Tuantranont A, et al. 3D-printed PLA/PEO blend as biodegradable substrate coating with CoCl2 for colorimetric humidity detection. Food Packag Shelf Life. 2022;32:100829.
21. Collazo-Bigliardi S, Ortega-Toro R, Chiralt A. Using lignocellulosic fractions of coffee husk to improve properties of compatibilised starch-PLA blend films. Food Packag Shelf Life. 2019;22:100423.
22. Kervran M, Vagner C, Cochez M, Ponçot M, Saeb MR, Vahabi H. Thermal degradation of polylactic acid (PLA)/ polyhydroxybutyrate (PHB) blends: a systematic review. Polym Degrad Stabil. 2022;201:109995.
23. Hernández-García E, Vargas M, Chiralt A. Effect of active phenolic acids on properties of PLA-PHBV blend films. Food Packag Shelf Life. 2022;33:100894.
24. Mishra S, Sahoo R, Unnikrishnan L, Ramadoss A, Mohanty S, Nayak SK. Enhanced structural and dielectric behaviour of PVDF-PLA binary polymeric blend system. Mater Today Commun. 2021;26:101958.
25. Hernández-López M, Correa-Pacheco ZN, Bautista-Baños S, Zavaleta-Avejar L, Benítez-Jiménez JJ, Sabino-Gutiérrez MA, et al. Bio-based composite fibers from pine essential oil and PLA/PBAT polymer blend. Morphological, physicochemical, thermal and mechanical characterization. Mater Chem Phys. 2019;234:345-53.
26. Sun H, Yang Z, Yang F, Wu W, Wang J. Enhanced simultaneous nitrification and denitrification performance in a fixed-bed system packed with PHBV/PLA blends. Int Biodeterior Biodegradation. 2020;146:104810.
27. Modi S, Koelling K, Vodovotz Y. Assessing the mechanical, phase inversion, and rheological properties of poly-[(R)-3-hydroxybutyrate-co-(R)-3-hydroxyvalerate] (PHBV) blended with poly-(l-lactic acid) (PLA). Eur Polym J. 2013;49(11):3681-90.
28. Gerard T, Budtova T. Morphology and molten-state rheology of polylactide and polyhydroxyalkanoate blends. Eur Polym J. 2012;48(6):1110-7.
29. Liu Q, Wu C, Zhang H, Deng B. Blends of polylactide and poly(3-hydroxybutyrate-co-3-hydroxyvalerate) with low content of hydroxyvalerate unit: morphology, structure, and property. J Appl Polym Sci. 2015;132(2):42689.
30. D'Anna A, Arrigo R, Frache A. PLA/PHB blends: biocompatibilizer effects. Polymers (Basel). 2019;11(9):1416.
31. Arrieta MP, Fortunati E, Dominici F, Rayón E, López J, Kenny JM. PLA-PHB/cellulose based films: mechanical, barrier and disintegration properties. Polym Degrad Stabil. 2014;107:139-49.
32. Hankermeyer CR, Tjeerdema RS. Reviews of environmental contamination and toxicology. Rev Environ Contam Toxicol. 1999;159:1-24.
33. Getachew A, Woldesenbet F. Production of biodegradable plastic by polyhydroxybutyrate (PHB) accumulating bacteria using low cost agricultural waste material. BMC Research Notes. 2016;9(1):1-9.
34. dos Santos AJ, Oliveira Dalla Valentina LV, Hidalgo Schulz AA, Tomaz Duarte MA. From obtaining to degradation of PHB: material properties. Part I. Ing Cienc. 2017;13(26):269-98.
35. Iulianelli GCV, Azevedo RDS, da Silva PSRC, Tavares MIB. PHB nanostructured: production and characterization by NMR relaxometry. Polym Test. 2016;49:57-65.
36. dos Santos FA, Iulianelli GCV, Bruno Tavares MI. Development and properties evaluation of bio-based PLA/PLGA blend films reinforced with microcrystalline cellulose and organophilic silica. Polym Eng Sci. 2017;57(4):464-72.
37. dos Santos FA, Iulianelli GCV, Tavares MIB. The use of cellulose nanofillers in obtaining polymer nanocomposites: properties, processing, and applications. Mater Sci Appl. 2016;07(05):257-94.
38. Iulianelli GCV, David GS, dos Santos TN, Sebastião PJO, Tavares MIB. Influence of TiO 2 nanoparticle on the thermal, morphological and molecular characteristics of PHB matrix. Polym Test. 2018;65:156-62.
39. Gong J, Li J, Xu J, Xiang Z, Mo L. Research on cellulose nanocrystals produced from cellulose sources with various polymorphs. RSC Advances. 2017;7(53):33486-93.
40. Rong MZ, Zhang MQ, Liu Y, Yang GC, Zeng HM. The effect of fiber treatment on the mechanical properties of unidirectional sisal-reinforced epoxy composites. Compos Sci Technol. 2001;61(10):1437-47.
41. Wang S, Qiaoli X, Fen L, Jinming D, Husheng J, Bingshe X. Preparation and properties of cellulose-based carbon microsphere/poly(lactic acid) composites. J Compos Mater. 2014;48(11):1297-302.
42. Inácio EM, Lima MCP, Souza DHS, Sirelli L, Dias ML. Crystallization, thermal and mechanical behavior of oligosebacate plasticized poly(lactic acid) films. Polímeros. 2018;28(5):381-8.
43. Mottin AC, Ayres E, Oréfice RL, Camada JJD. What changes in Poly(3- Hydroxybutyrate) (PHB) when processed as electrospun nanofibers on thermo-compression molded film. Mater Res. 2016;19:57-66.
44. Zhang M, Thomas NL. Blending polylactic acid with polyhydroxybutyrate: the effect on thermal, mechanical, and biodegradation properties. Adv Polym Technol. 2011;30(2):67-79.
45. Burgos N, Martino VP, Jiménez A. Characterization and ageing study of poly(lactic acid) films plasticized with oligomeric lactic acid. Polym Degrad Stabil. 2013;98(2):651-8.
46. Farid T, Herrera VN, Kristiina O. Investigation of crystalline structure of plasticized poly(lactic acid)/Banana nanofibers composites. IOP Conf Ser.: Mater Sci Eng. 2018;369:012031.
47. Gong M, Zhao Q, Dai L, Li Y, Jiang T. Fabrication of polylactic acid/ hydroxyapatite/graphene oxide composite and their thermal stability, hydrophobic and mechanical properties. J Asian Ceram Soc. 2017;5(2):160-8.
48. Furukuwa T, Sato H, Murakami R, Zhang J, Duan YX, Noda I, et al. Structure, dispersibility, and crystallinity of Poly(hydroxybutyrate)/Poly(l-lactic acid) blends studied by FT-IR microspectroscopy and differential scanning calorimetry. Macromolecules. 2005;38(15):6445-54.
49. Hu Y, Sato H, Zhang J, Noda I, Ozak IY. Crystallization behavior of poly(l-lactic acid) affected by the addition of a small amount of poly(3-hydroxybutyrate). Polymer (Guildf). 2008;49(19):4204-10.

50. Zhang M, Thomas NL. Blending polylactic acid with polyhydroxybutyrate: the effect on thermal, mechanical, and biodegradation properties. Adv Polym Technol. 2011;30:67-79.
51. Abdelwahab MA, Flynn A, Chiou BS, Imam S, Orts W, Chiellini E. Thermal, mechanical and morphological characterization of plasticized PLA-PHB blends. Polym Degrad Stabil. 2012;97:1822-8.
52. Arrieta MP, Samper MD, López J, Jiménez A. Combined effect of poly(hydroxybutyrate) and plasticizers on polylactic acid properties for film intended for food packaging. J Polym Environ. 2014;22:460-70.
53. Battegazzore D, Bocchini S, Frache A. Crystallization kinetics of poly(lactic acid)-talc composites. Express Polym Lett. 2011;5(10):849-58.
54. Restrepo I, Medina C, Meruane V, Akbari-Fakhrabadi A, Flores P, Rodríguez-Llamazares S. The effect of molecular weight and hydrolysis degree of poly(vinyl alcohol) (PVA) on the thermal and mechanical properties of poly(lactic acid)/PVA blends. Polímeros. 2018;28(2):169-77.
55. Wellen RMR, Canedo EL, Rabello MS. Melting and crystallization of poly(3-hydroxybutyrate)/carbon black compounds. Effect of heating and cooling cycles on phase transition. J Mater Res. 2015;30(21):3211-26.
56. Xu P, Luo X, Zhou Y, Yang Y, Ding Y. Enhanced cold crystallization and dielectric polarization of PLA composites induced by P[MPEGMA-IL] and graphene. Thermochim Acta. 2017;657:156-62.
57. Kervran M, Vagnera C, Cochez M, Ponçot M, Saeb MR, Vahabi H. Thermal degradation of polylactic acid (PLA)/ polyhydroxybutyrate (PHB) blends: a systematic review. Polym Degrad Stabil. 2022;201:109995.
58. Monteiro MSSB, Cucinelli RP No, Santos ICS, da Silva EO, Tavares MIB. Inorganic-organic hybrids based on poly (ε-caprolactone) and silica oxide and characterization by relaxometry applying low-field NMR. Mater Res. 2012;15(6):825-32.
59. Besghini D, Mauri M, Simonutti R. Time Domain NMR in polymer science: from the laboratory to the industry. Appl Sci (Basel). 2019;9(9):1801.
60. Almeida AS, Tavares MIB, da Silva EO, Cucinelli RP No, Moreira LA. Development of hybrid nanocomposites based on PLLA and low-field NMR characterization. Polym Test. 2012;31(2):267-75.